# Efficient search for new physics using Active Learning in the ATLAS Experiment

**Irina Espejo[1] and Patrick Rieck[1] on behalf of the ATLAS Collaboration**

[1]New York University

E-mail: iem244@nyu.edu

**Abstract.** Searches for new physics at the LHC set exclusion limits in multi-dimensional parameter spaces of various theories. Typically, these are presented as 1- or 2-dimensional parameter scans; however, the relevant theory's parameter space is usually of a higher dimension. As a result only a subspace is covered, which is due to the exponential computing requirements of simulations for scattering processes of interest. An Active Learning approach using a Gaussian Process is presented to address this limitation. Compared to the usual grid scan, this iterative procedure reduces the number of points in parameter space for which exclusion limits need to be determined. The Active Learning procedure is applied to a dark matter search performed by the ATLAS experiment, extending its interpretation from a 2 to a 4-dimensional parameter space while keeping the computational effort at a low level.

## 1. Introduction

The Large Hadron Collider (LHC) and the ATLAS experiment [1] aim to find evidence for physics Beyond the Standard Model (BSM)[1]. Theoretical BSM models often include multiple parameters that need to be constrained by the experimental data. Due to computational limitations, traditional approaches search over only one or two parameters, neglecting the potential for excluding large volumes of the parameter space.

In Ref. [2], a new and efficient approach is proposed based on Active Learning. The method is iterative and selects parameter points based on their proximity to the exclusion contour, as predicted by a surrogate Gaussian Process model. The selected BSM points are then evaluated to obtain upper limits on the signal strength. The limit evaluation and physics details are handled using the RECAST protocol [2, 3] from a previous analysis. As evaluating the full analysis pipeline is computationally demanding, the method leverages the availability of SimpleAnalysis data, which provides a simplified version of the RECAST pipeline. The scalability of the method is demonstrated using a reinterpretation of a search for Dark Matter produced in association with a SM Higgs boson decaying into b-quarks. The paper is organized into the following sections, including an overview of the signal model, a description of the evaluation of SimpleAnalysis and RECAST pipelines, a description of the methodology, and a discussion of the results and conclusions.

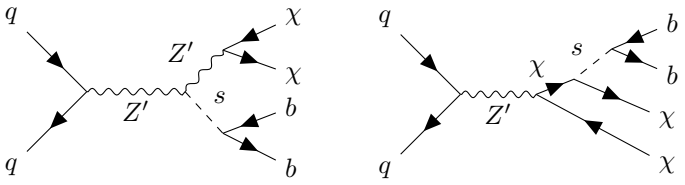


**Figure 1.** Tree-level Feynman diagrams of the production of a Dark Higgs boson $s$ together with a pair of Dark Matter particles $\chi$, mediated by a $Z'$ particle which also interacts with the initial state quarks.

## 2. Building blocks

### *2.1. Mono-H($b\bar{b}$) search*

In this study, the Mono-H($b\bar{b}$) search is reinterpreted [4, 5] within the framework of a new model which involves a Dark Higgs boson [6], decaying into $b\bar{b}$ and interacting with a $Z'$ boson that decays into two Dark Matter particles $\chi$ (Feynman diagram in Fig. 1). The parameters of this model are the mass of the Dark Higgs $m_s$, the mass of the $Z'$ boson $m_{Z'}$, the mass of the Dark Matter particle $m\chi$, and the coupling constant $g_\chi$ between the $Z'$ boson and Dark Matter $\chi$. The coupling constant, $g_q$, has been fixed at 0.25. The experimental signatures of this model at the LHC can be observed through missing transverse momentum $E_{\mathrm{T}}^{\mathrm{miss}}$ and the presence of at least two jets containing $B$-hadron decay products. The invariant mass of the $B$-hadrons are not restricted to the SM Higgs but can range from 50-280 GeV. The main backgrounds for this signal include the SM production of a Higgs boson and the production of a $Z$ boson in association with jets, with the Z decaying into neutrinos, as well as further reducible backgrounds. Briefly, the signal region is defined as $E_{\mathrm{T}}^{\mathrm{miss}} > 150$ GeV and no leptons, while the control region is similar but allows for one or two leptons.

### *2.2. Active Learning*

Active learning [7] is an iterative machine learning technique in which an agent is able to interactively select and label data points for the training of a downstream task. This technique is particularly useful when the training dataset is scarce and the labeling process is costly or time-consuming. The goal of Active Learning is to accomplish the task with the minimum number of labels possible. Interactive querying allows spending resources only on labeling the most informative samples for the downstream task. The selection of data samples for labeling involves a trade-off between exploration and exploitation, which is encoded in an acquisition function. In this reinterpretation, the downstream task is the classification of new physics parameter points $\boldsymbol{\theta} = (m_{Z'}, m_s, m_\chi, g_\chi)$ as excluded or non-excluded by the Mono-H($b\bar{b}$) search. The exclusion contour is delimited by the logarithm of the upper limit on the Dark Higgs boson signal strength, $\mu^{\text{Upper Limit}} \equiv \left(\frac{\sigma^{\text{Upper Limit}}}{\sigma_{\text{SM}}}\right)$, as seen in Equation 1.

$$f(\boldsymbol{\theta}) = \log\left(\mu^{\text{Upper Limit}}\right) \tag{1}$$

The usual CLs procedure is used to determine $f(\boldsymbol{\theta})$. Regions outside the 95% CL upper limit are given by the exclusion contour of interest $\{\boldsymbol{\theta} \in \mathbb{R}^4 \,|\, f(\boldsymbol{\theta}) = 0\}$.

### *2.3. SimpleAnalysis and RECAST pipelines*

In this section, both modes of parameter point evaluation for limit setting are detailed.

**SimpleAnalysis** (*Low fidelity*). A simplified implementation of the Mono-H($b\bar{b}$) search has been implemented using the SimpleAnalysis framework [8]. The implementation enables the fast evaluation of a large number of different configurations of the model under study by simulating the signal process without considering the detector response in detail. Detector simulation is usually the most computationally-expensive part of a new physics search analysis. SimpleAnalysis provides simplified implementations of detector response, physics object reconstruction, and event

selection. For more details about the SimpleAnalysis implementation see Ref. [2].

**RECAST workflow** (*High fidelity*). Obtaining new upper limits on signal strength according to this reinterpretation of the Mono-H($b\bar{b}$) consists of two parts. In the first part, for a given parameter query, configuration files are prepared for the Monte Carlo simulation of the signal scattering process. In the second step, event generation and full simulation of the detector using GEANT4 [9]. Lastly, limits are computed using CERN's REANA platform [10] using the RECAST protocol [3, 11].

## 3. Related Work

Previous studies in Active Learning for Beyond the Standard Model (BSM) interpretations in High Energy Physics (HEP) utilizing LHC data have been limited to either predetermined results [12] or rough exclusion limits [13]. In contrast, the current study integrates Active Learning into a complete and accurate physics analysis procedure. This allows for new data requests to trigger the execution of the analysis pipeline, leading to accurate exclusion limits obtained through the automation of the preserved analysis workflow. Here, we take the proposal of Ref. [14] and develop it in the context of a real, full search analysis.

## 4. Proposed method

Active Learning has two main ingredients: a surrogate model to interpolate between data points and an acquisition function to decide which data points should be labeled next.

### *4.1. Warm start*

The first iteration of Active Learning begins with no RECAST (high-fidelity) points. To ensure that the first query is informed, the parameter space is populated using SimpleAnalysis (low-fidelity) data. This data is then used to fit an out-of-the-box Gaussian Process. This approach is referred to as "warm start".

### *4.2. Surrogate model*

The surrogate model in this application must have: 1) the ability to leverage large low-fidelity data (∼5000 points) for physical predictions, 2) the capacity to make predictions using a few high-fidelity data points (<1000), 3) an inherent concept of uncertainty and 4) interpretable parameters/components for physics-based constraints. We select a 2-task Multitask Gaussian Process (GP) [15] where the first task is regression over SimpleAnalysis (low fidelity) data points $\mathcal{D}_{SA} = \{\boldsymbol{\theta}^i_{SA}, y^i_{SA}\}_i$ and the second task is regression over RECAST (high fidelity) data points $\mathcal{D}_{reco} = \{\boldsymbol{\theta}^i_{reco}, y^i_{reco}\}_i$. The Gaussian Process mean $m(\boldsymbol{\theta})$ and kernel $k(\boldsymbol{\theta}, \boldsymbol{\theta}')$ and its corresponding hyperparameters are given by

$$m(\boldsymbol{\theta}) = \boldsymbol{w}^T\boldsymbol{\theta} + b \ , \ w \in \mathbb{R}^4 \ , b \in \mathbb{R}$$

$$k_{ij}(\boldsymbol{\theta}, \boldsymbol{\theta}') = k(\boldsymbol{\theta}, \boldsymbol{\theta}')\kappa_{ij} + \epsilon^2\delta(\boldsymbol{\theta}, \boldsymbol{\theta}') \ , \quad \delta(\boldsymbol{\theta}, \boldsymbol{\theta}') = \begin{cases} 1, & \text{if } \ \boldsymbol{\theta} = \boldsymbol{\theta}' \\ 0, & \text{else} \end{cases} \ ,$$

$$k(\boldsymbol{\theta}, \boldsymbol{\theta}') = \exp\left(-\frac{||\boldsymbol{\theta} - \boldsymbol{\theta}'||^2}{2\,l^2}\right), \ \ l \in \mathbb{R}$$

$$k_{ij} = \begin{cases} \sigma_{SA} \text{ if } i = j = 1 \\ \sigma_{reco} \text{ if } i = j = 2 \\ \sigma_{sr} \text{ if } i \neq j \end{cases}$$

In both tasks, the Multitask GP uses the same mean function. This, and the kernel selection, allows the low-fidelity data to inform the high-fidelity regression where there is a lack of high-fidelity data. The linear mean was chosen because it aligns with the pre-known monotonicity of the Confidence Level surface in certain directions. The Hadamard Multitask Kernel [15] was selected for its simplicity and ability to account for correlation between tasks.

*4.3. Acquisition Function*

The goal is to find the contour $y_{reco}(\boldsymbol{\theta}) = 0$ up to a certain accuracy with as few queries as possible. The acquisition function $a(\boldsymbol{\theta})$ used here is a variant of Maximum Entropy Search (MES) from Bayesian Optimization (BO) [16] but with the added challenge that we are looking for a level set and not a single point like in BO. This acquisition function queries those parameter points where its exclusion status is most uncertain, i.e. those closer to the current predicted contour. The exclusion probability for a parameter space point is

$$p_{\text{excl}}\left(\boldsymbol{\theta}\right) = \int_{-\infty}^{0} g\left(y \,|\, \mu(\boldsymbol{\theta}),\, \sigma(\boldsymbol{\theta})\right) dy \tag{2}$$

This exclusion probability is turned into the exclusion entropy over the exclusion contour,

$$H_{\text{excl}}(\boldsymbol{\theta}) = -p_{\text{excl}}(\boldsymbol{\theta}) \log p_{\text{excl}}(\boldsymbol{\theta}) - (1 - p_{\text{excl}}(\boldsymbol{\theta})) \log\left(1 - p_{\text{excl}}(\boldsymbol{\theta})\right) \tag{3}$$

The acquisition function that minimizes exclusion entropy in Equation 3 was determined to be too computationally intensive for the task of finding four contours, namely the expected limit, the observed limit, and the $\pm 1\sigma$ bands around the expected limit. For simplicity, only expected limit data is used to compute the acquisition function. It is assumed that the four contours are relatively close to each other in the 4D parameter space so that points close to the contour on the expected limit surface ($y_{exp}(\boldsymbol{\theta}) \approx 0$) are relatively close to the observed limit contour ($y_{obs}(\boldsymbol{\theta}) \approx 0$) although not queried to be optimal.

To account for the lack of exploration of MES, Poisson-disc sampling [17] bounded by two times the standard deviation of the expected exclusion contour $\bar{y}_{exp}(\boldsymbol{\theta})$ is also used in the acquisition function. In order to maximize the benefits of parallel evaluation and recasting, it is recommended to query a batch of $q$ points instead of a single point at a time. Half of each batch was acquired through MES and the other half through Poisson-disc sampling.

**Algorithm 1** Method to efficiently obtain 4D exclusion contours

**Warm start input:** Initial dataset SimpleAnalysis (low fidelity) $\mathcal{D}_{SA}$, an out-of-the-box Gaussian Process $f$, an acquisition function $a(\boldsymbol{\theta})$
Train $f$ on $\mathcal{D}_{SA}$
Select next $q$-batch $\{\boldsymbol{\theta}_1, ..., \boldsymbol{\theta}_q\}$ according to acquisition function $a(\boldsymbol{\theta})$
Evaluate $\{\boldsymbol{\theta}^1, ..., \boldsymbol{\theta}^q\}$ on RECAST (high fidelity)
**Warm start output:** Datasets $\mathcal{D}_{SA}$, $\mathcal{D}_{reco,1} = \{(\boldsymbol{\theta}^i, y^i_{reco})\}_{i=1..q}$
**Active Learning input:** Initial datasets $\mathcal{D}_{SA}$, $\mathcal{D}_{reco,1}$ , a 2-task Multitask Gaussian Process $g$, an acquisition function $a(\boldsymbol{\theta})$
$D_{SA} \leftarrow$ Initial dataset for task 1
$D_{reco,1} \leftarrow$ Initial dataset for task 2
**for** $j = 1$ to $n$ **do**
    Train $f$ on $D_{SA}$ and $D_{reco,j}$
    Select next batch $\{\boldsymbol{\theta}^1_j, ..., \boldsymbol{\theta}^q_j\}$ according to acquisition function $a(\boldsymbol{\theta})$
    Evaluate $\{\boldsymbol{\theta}^1_j, ..., \boldsymbol{\theta}^q_j\}$ on RECAST (high fidelity)
    Add batch $\{\boldsymbol{\theta}^1_j, ..., \boldsymbol{\theta}^q_j\}$ and its evaluations to $D_{reco,j+1}$
**end for**
**return** $D_{SA}$, $D_{reco,n}$, $f$
**Active Learning output:** Final datasets $D_{SA}$, $D_{reco,n}$, $f$

## 5. Results

In accordance with the procedure outlined in Algorithm 1, four iterations of Active Learning were performed by querying the high-fidelity RECAST pipeline, each with a batch of approximately 200 parameter points. The parameter space consists of $m_{Z'} \in [500, 5000]$ GeV, $m_s \in [50, 150]$ GeV, $m_\chi \in [100, 1200]$ GeV, and $g_\chi \in [0.5, 2.0]$. A total of approximately 800 high-fidelity points and 5000 low-fidelity SimpleAnalysis points were used. Each batch of 200 points, ran on CERN's computational facilities, took 1 week to process due to the computation of Monte Carlo event generation, coordination among analyzers, and the coordination between Monte Carlo experts. The Multitask GP fits were implemented in `GPyTorch` [18] carried out on a V100 NVIDIA GPU with 32GB of RAM. After the last iteration, the Multitask GP posterior for the RECAST task (high-fidelity) provides the expected and observed 4D limit contours for any combination of parameters. For visualization, 2D projections are shown in Figure 2. Further projections and evaluation metrics can be found in Appendix A.

## 6. Conclusion

In this paper, we demonstrate that by combining Active Learning and RECAST, it is possible to efficiently estimate and scale exclusion limits under a limited computational budget. A 4D exclusion contour was obtained, an improvement from the traditional brute force approach used in 2D or 1D exclusion contours. The analysis is a reinterpretation of the Mono-H($b\bar{b}$) Dark Matter search at the LHC using the ATLAS detector[1], which analyzes the signatures of two b-jets and missing transverse momentum, a signature in exploring extensions of the Standard Model. Our study covers multiple regimes without any approximations. The methodology used is not strongly tailored to the Dark Higgs model and instead relies on RECAST to handle the physics aspect of the analysis. The aspect that may require some adaptation for other analyses is the design of the Gaussian Process mean and kernel but keeping the Multitask aspect to leverage SimpleAnalysis data or other low-fidelity data, like those in cross-section measurements.

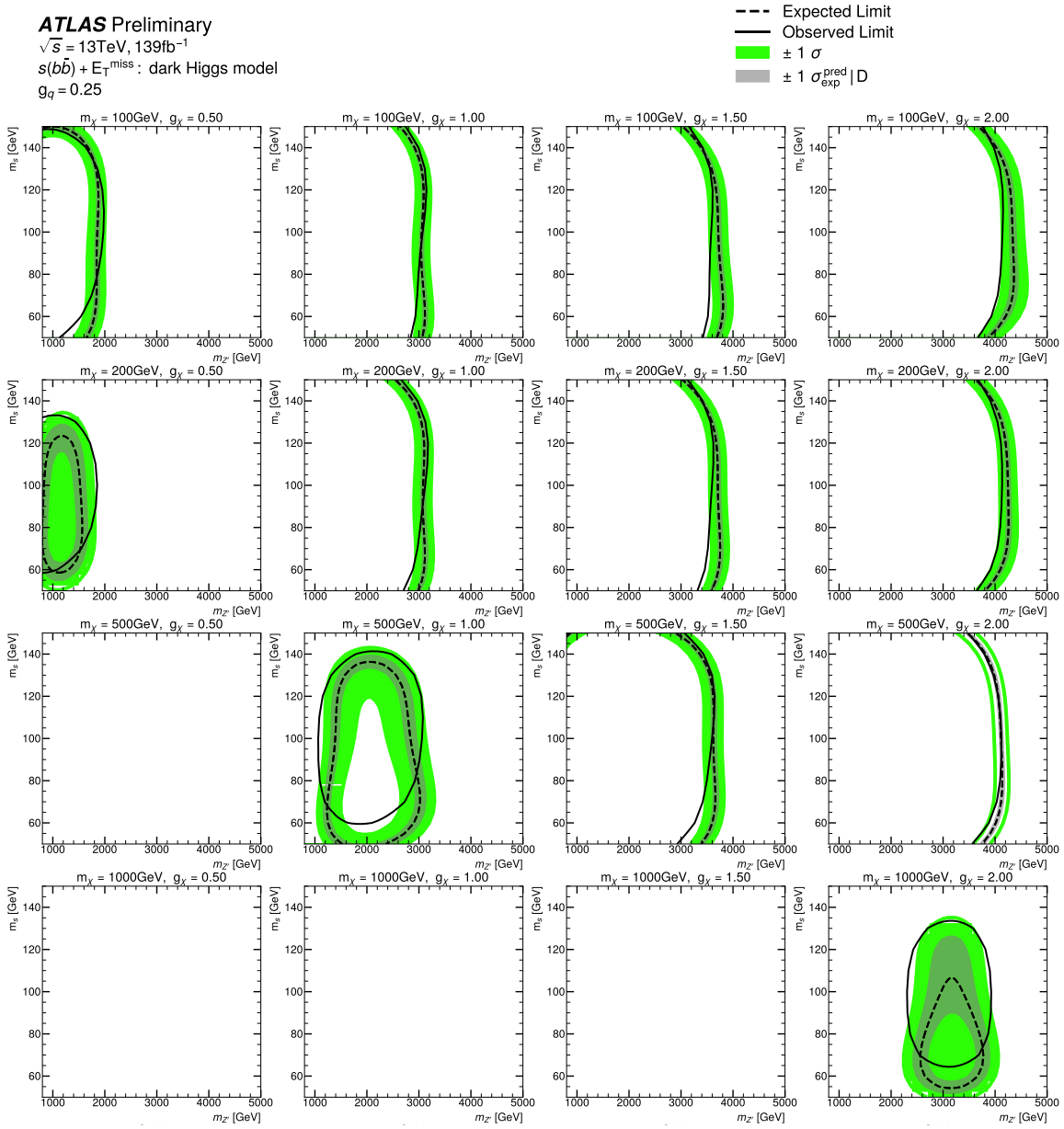


**Figure 2.** Exclusion limits on the mediator mass $m_{Z'}$ and $m_s$ where $g_q$=0.25 and each slice corresponds to a fixed value for $m_\chi$ and $g_\chi$ [2]. The regions to the left of the contours are excluded. The exclusion limits are determined by evaluating the Multitask GP in a four-dimensional grid. The blank figures in the lower left corner are included for completeness, demonstrating that large dark matter masses and low coupling strengths are not excluded.

## Appendix A. More plots of the 4D exclusion contour

Figure A1 shows another view of the 4D contour in Figure 2. Exclusion entropy can be used

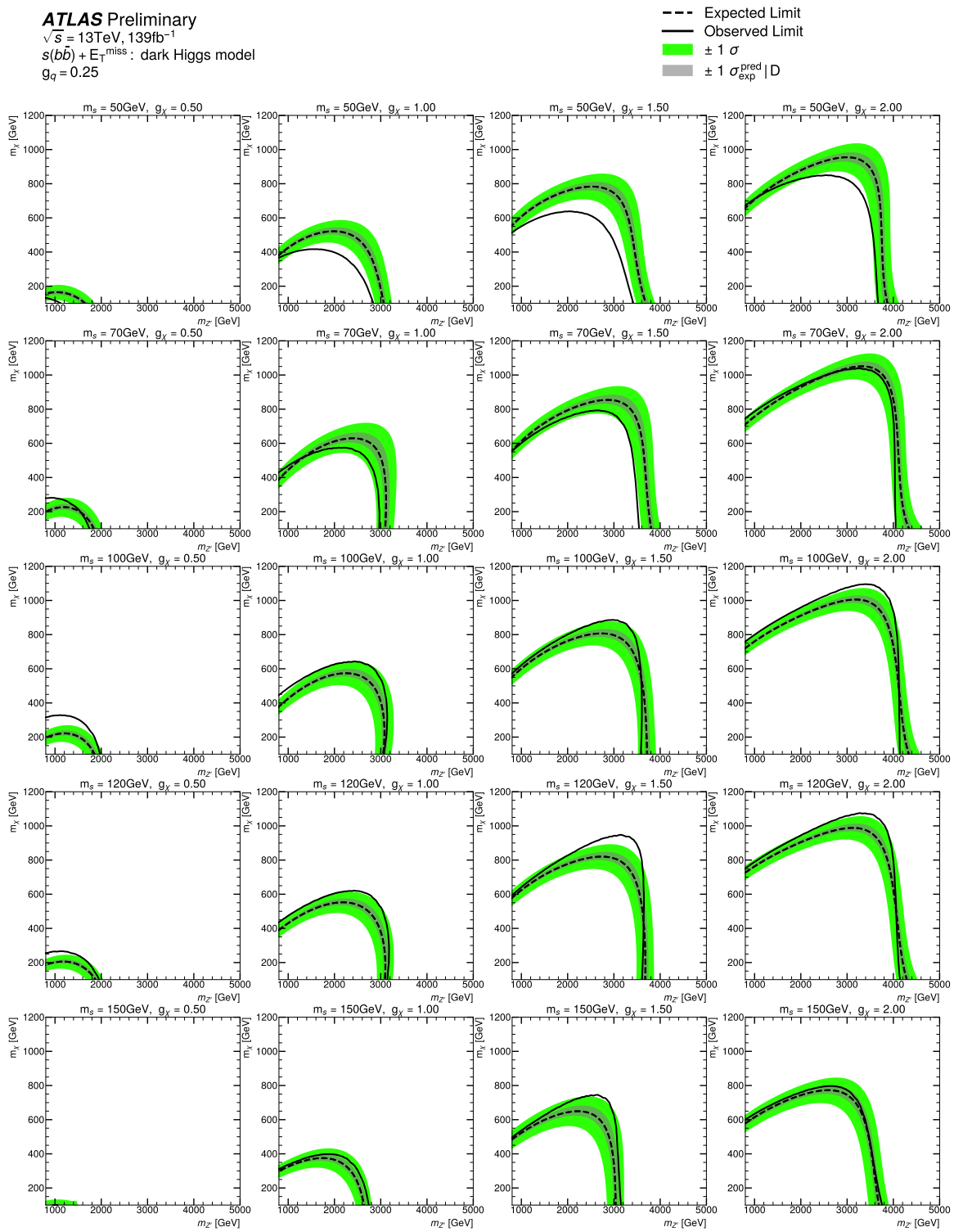


**Figure A1.** Exclusion limits on the mediator masses $m_{Z'}$ and $m_s$ where $g_q$=0.25 and each slice corresponds to a fixed value for $m_s$ and $g_\chi$ [2].

as a metric to assess the progress of the method. Ideally, entropy should be zero everywhere in the parameter space except for a sharp concentration of high entropy around the true contour. This means that uncertainty about the exclusion is zero almost everywhere except close to the contour, where entropy can never really disappear due to the continuous nature of estimating a curve with a finite number of queries. See entropy maps of Figures 2 and A1 in Figures A2 and A3, respectively.

## References


[1] ATLAS Collaboration. The ATLAS Experiment at the CERN Large Hadron Collider. *JINST*, 3:S08003, 2008. doi:10.1088/1748-0221/3/08/S08003.

[2] ATLAS Collaboration. ATL-PHYS-PUB-2022-045. Active Learning reinterpretation of an ATLAS Dark Matter search constraining a model of a dark Higgs boson decaying to two b-quarks, 2022. URL: https://atlas.web.cern.ch/Atlas/GROUPS/PHYSICS/PUBNOTES/ATL-PHYS-PUB-2022-045/.

[3] Kyle Cranmer and Itay Yavin. RECAST — extending the impact of existing analyses. *Journal of High Energy Physics*, 2011(4):38. doi:10.1007/JHEP04(2011)038.

[4] ATLAS Collaboration. Constraints on mediator-based dark matter and scalar dark energy models using $\sqrt{s} = 13$ tev $pp$ collision data collected by the ATLAS detector. *Journal of High Energy Physics*, 2019(5):142, 2019. doi:10.1007/JHEP05(2019)142.

[5] ATLAS Collaboration. EXOT-2020-04. Search for dark matter produced in association with a dark Higgs boson decaying to $W^+W^-$ in the one-lepton final state at $\sqrt{s} = 13$TeV using 139fb$^{-1}$ of $pp$ collisions recorded with the ATLAS detector, 2020. URL: https://atlas.web.cern.ch/Atlas/GROUPS/PHYSICS/PAPERS/EXOT-2020-04/.

[6] Michael Duerr, Alexander Grohsjean, Felix Kahlhoefer, Bjoern Penning, Kai Schmidt-Hoberg, and Christian Schwanenberger. Hunting the dark Higgs. *Journal of High Energy Physics*, 2017(4):143. doi:10.1007/JHEP04(2017)143.

[7] D. A. Cohn, Z. Ghahramani, and M. I. Jordan. Active Learning with Statistical Models. *Journal of Artificial Intelligence Research*, 4:129–145, 1996. URL: https://www.jair.org/index.php/jair/article/view/10158, doi:10.1613/jair.295.

[8] ATLAS Collaboration. ATL-PHYS-PUB-2022-017. SimpleAnalysis: Truth-level analysis framework. 2022. URL: https://atlas.web.cern.ch/Atlas/GROUPS/PHYSICS/PUBNOTES/ATL-PHYS-PUB-2022-017/.

[9] J. Allison et. al. Recent developments in Geant4. *Nuclear Instruments and Methods in Physics Research Section A: Accelerators, Spectrometers, Detectors and Associated Equipment*, 835:186–225, 2016. doi:10.1016/j.nima.2016.06.125.

[10] Tibor Šimko, Lukas Heinrich, Harri Hirvonsalo, Dinos Kousidis, and Diego Rodríguez. REANA: A System for Reusable Research Data Analyses. *EPJ Web of Conferences*, 214:06034, 2019. doi:10.1051/epjconf/201921406034.

[11] Kyle Cranmer, Lukas Heinrich, and on behalf of the ATLAS collaboration. Analysis Preservation and Systematic Reinterpretation within the ATLAS experiment. *Journal of Physics: Conference Series*, 1085(4):042011, 2018. doi:10.1088/1742-6596/1085/4/042011.

[12] Heskes T. Otten S. et al. Caron, S. Constraining the parameters of high-dimensional models with active learning. *Eur. Phys. J. C 79, 944*. URL: https://doi.org/10.1140/epjc/s10052-019-7437-5.

[13] Juan Rocamonde, Louie Corpe, Gustavs Zilgalvis, Maria Avramidou, and Jon Butterworth. Picking the low-hanging fruit: Testing new physics at scale with active learning. *SciPost Physics*, 13(1). doi:10.21468/SciPostPhys.13.1.002.

[14] L. Heinrich, G. Louppe, and Cranmer. Excursion Set Estimation using Sequential Entropy Reduction for Efficient Searches for New Physics at the LHC. In *Advanced Computing and Analysis Techniques in Physics Research*, 2019. URL: https://indico.cern.ch/event/708041/contributions/3269754/.

[15] Edwin V Bonilla, Kian Chai, and Christopher Williams. Multi-task Gaussian Process Prediction. In *Advances in Neural Information Processing Systems*, volume 20. Curran Associates, Inc., 2007. URL: https://papers.nips.cc/paper/2007/hash/66368270ffd51418ec58bd793f2d9b1b-Abstract.html.

[16] Zi Wang and Stefanie Jegelka. Max-value Entropy Search for Efficient Bayesian Optimization, 2018. arXiv:1703.01968.

[17] Manohar Vanga. Poisson Disk Sampling in Processing, 2023-02-03. URL: https://sighack.com/post/poisson-disk-sampling-bridsons-algorithm.

[18] Jacob R. Gardner, Geoff Pleiss, David Bindel, Kilian Q. Weinberger, and Andrew Gordon Wilson. GPyTorch: Blackbox Matrix-Matrix Gaussian Process Inference with GPU Acceleration, 2021. arXiv:1809.11165, doi:10.48550/arXiv.1809.11165.

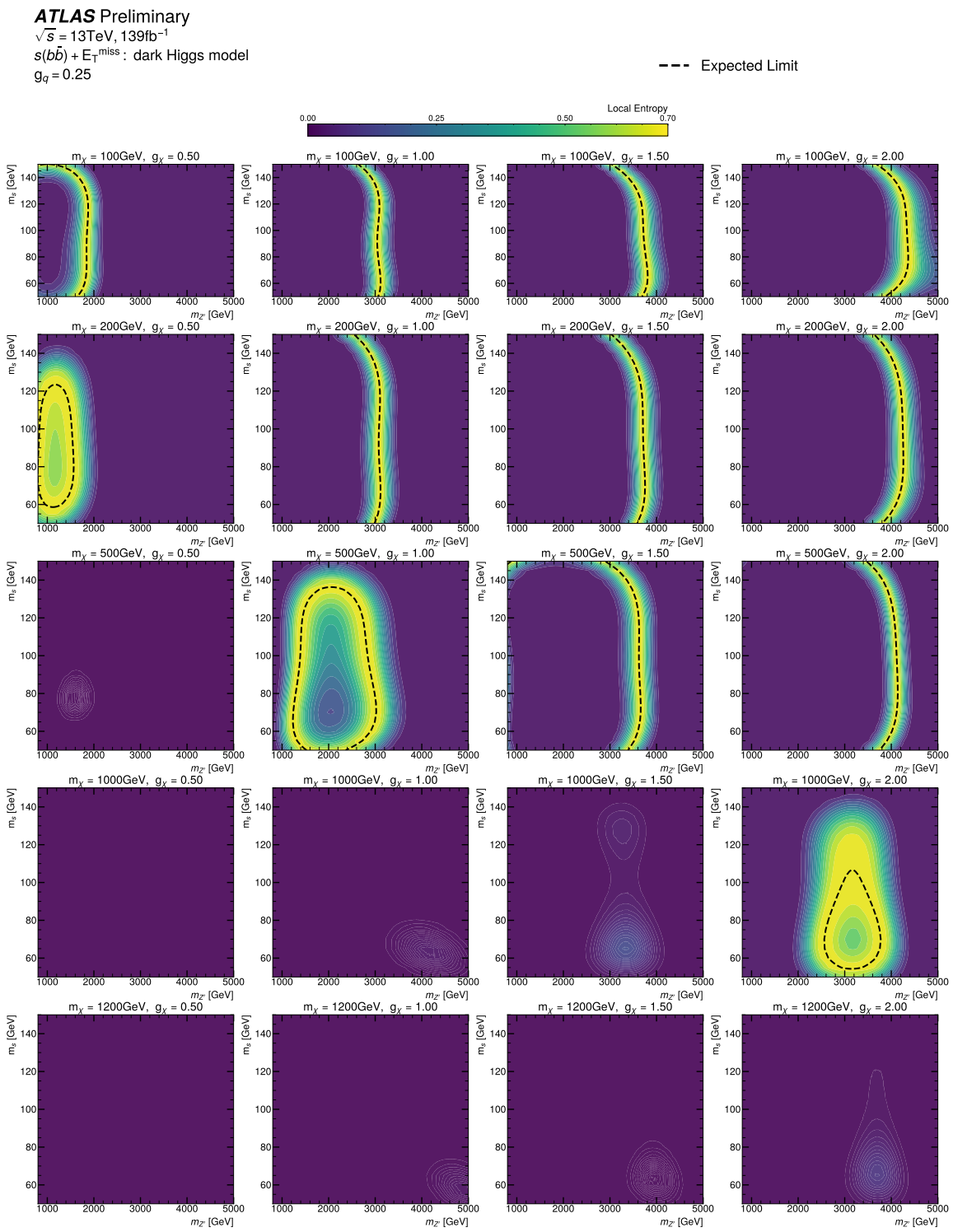


**Figure A2.** Exclusion entropy according to the posterior distribution of the final Multitask GP in 4D for the projection in Figure 2 [2].

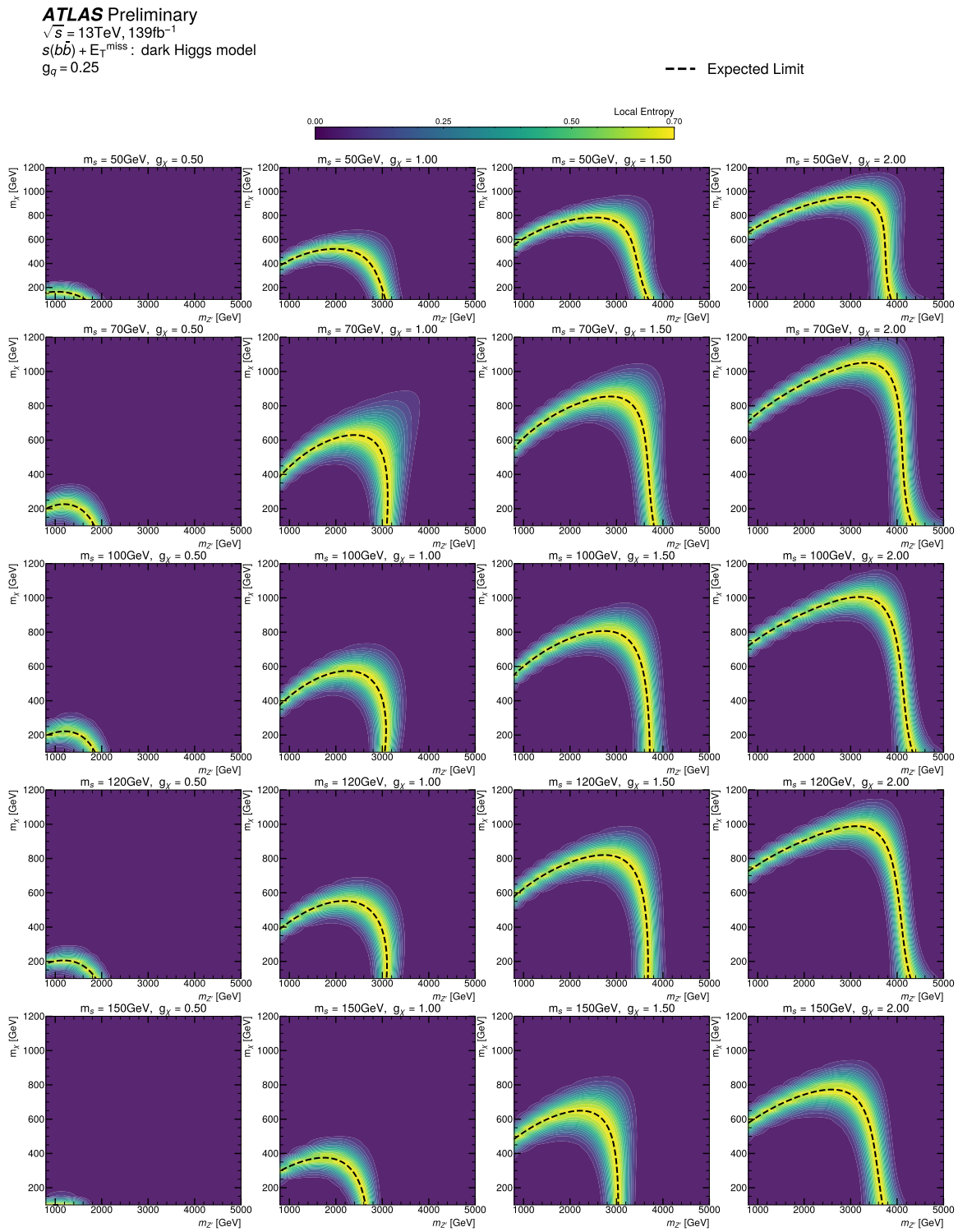


**Figure A3.** Exclusion entropy according to the posterior distribution of the final Multitask GP in 4D for the projection in Figure A1 [2].